phys. stat. sol. (b) **218**, 379 (2000)

Subject classification: 61.43.Fs; 64.60.Qb; 64.70.Pf; S8.12

A Theoretical Study on Thermo-Analytical Techniques in Differential Scanning Calorimetry. Application to the Crystallization of the Semiconducting $Sb_{0.12}As_{0.40}Se_{0.48}$ Alloy

P. L. LÓPEZ-ALEMANY, J. VÁZQUEZ, P. VILLARES, and R. JIMÉNEZ-GARAY

Departamento de Física de la Materia Condensada, Facultad de Ciencias, Universidad de Cádiz, Apartado 40, 11510 Puerto Real (Cádiz), Spain

(Received February 19, 1999; in revised form August 4, 1999)

A procedure has been developed for analyzing the evolution with time of the volume fraction crystallized and for calculating the kinetic parameters at non-isothermal reactions in materials involving formation and growth of nuclei. Considering the assumptions of extended volume and random nucleation, a general expression of the fraction crystallized as a function of time has been obtained in isothermal crystallization process. The application of the crystallization rate to the non-isothermal processes has been carried out under the restriction of a nucleation which takes place early in the transformation and the nucleation frequency is zero thereafter. Under these conditions, the kinetic parameters have been deduced by using the techniques of data analysis of single-scan and multiple-scan. The theoretical method developed has been applied to the crystallization kinetics of the semiconducting $Sb_{0.12}As_{0.40}Se_{0.48}$ alloy. The kinetic parameters obtained according to both techniques differ by only about 6%, which confirms the reliability and accuracy of the single-scan technique when calculating the above-mentioned parameters in non-isothermal crystallization processes.

1. Introduction

Although glass has been used as an artistic medium and industrial material for centuries it has been only in recent years that "glass science" has emerged as a field of study in its own right. The advances that have been made in the physics and chemistry of these materials have been widely appreciated within the research community. A strong theoretical and practical interest in the application of isothermal and non-isothermal experimental analysis techniques to the study of phase transformations has been developed in the last decades. The non-isothermal thermo-analytical techniques have become particularly prevalent for the investigation of the processes of nucleation and growth that occur during transformation of the metastable phases in the glassy alloy as it is heated. These techniques provide rapid information on such parameters as glass transition temperature, transformation enthalpy and activation energy over a wide range of temperature [1]. In addition, the high thermal conductivity as well as the temperature at which transformations occur in most amorphous alloys make these transformations particularly suited to analysis in a differential scanning calorimeter (DSC).

The study of crystallization kinetics in amorphous materials by DSC methods has been widely discussed in the literature [2, 3]. There is a large variety of mathematical treatments mostly based on the Johnson-Mehl-Avrami (JMA) transformation rate equa-

tion [4, 5]. In this work the conditions of applicability of the JMA transformation rate equation to non-isothermal crystallization are established. The kinetic parameters of the above-mentioned crystallization are deduced by using the techniques of data analysis of single-scan and multiple-scan. Finally, the present paper applies the quoted techniques to the analysis of the crystallization kinetics of the glassy alloy $Sb_{0.12}As_{0.40}Se_{0.48}$ and the values of the kinetic parameters thus obtained differ by about 6%. This fact shows the reliability and accuracy of the single-scan technique for the calculation of the quoted parameters from a continuous heating treatment.

2. Theoretical Basis

Crystallization is a particular case of nucleation and grain growth controlled solid-state transformation processes, the theory of which is well known [4 to 7]. If an embryo of the transformed phase nucleates at moment τ and grows thereafter, in general, anisotropically with principal growth velocities, $u_i(t')$ ($i = 1, 2, 3$), in three mutually perpendicular directions, then its volume v at moment t (where $\tau < t' < t$) is

$$v(\tau, t) = g \prod_i \int_\tau^t u_i(t')\, \mathrm{d}t' , \tag{1}$$

where g is a geometric factor which depends on the shape of the growing crystal and the expression $\prod_i \int_\tau^t u_i(t')\, \mathrm{d}t'$ condenses the product of the integrals corresponding to the values of the above quoted subscript i.

When the overlap of the grains is neglected, it is possible to define an extended volume of transformed material, and assuming spatially random nucleation, according to literature [8] results

$$x(t) = 1 - \exp\left\{ -g \int_0^t I_v(\tau) \left[\prod_i \int_\tau^t u_i(t')\, \mathrm{d}t' \right] \mathrm{d}\tau \right\} \tag{2}$$

the basic nucleation-growth equation for the transformed fraction x. If the crystal growth rate is isotropic, $u_i(t') = u(t')$, an assumption which is in agreement with the experimental evidence, since in many transformations the reaction product grows approximately with the same rate in all directions, the Eq. (2) can be written as

$$x(t) = 1 - \exp\left[-g \int_0^t I_v(\tau) \left(\int_\tau^t u(t')\, \mathrm{d}t' \right)^m \mathrm{d}\tau \right] . \tag{3}$$

Here m is an integer or half integer which depends on the mechanism of growth and the dimensionality of the crystal. For interface-controlled growth or diffusion-controlled growth with u independent of time, m assumes the values, 1, 2 and 3 for one- two- and three-dimensional growth, respectively. For diffusion-controlled growth where u decreases as $t^{-1/2}$, m assumes the values 1/2, 1 and 3/2 for the respective dimensionalities of growth.

Equation (3) is evidently valid under any thermal conditions. Up to this point no assumptions have been made regarding the origin of the time dependence of I_v and u. An important limitation of this equation, however, stems from the condition of a completely random overlap of growing crystallites.

For the important case of isothermal crystallization with nucleation frequency and growth rate independent of time, Eq. (3) can be integrated yielding an expression, that can be taken as a detailed specific case of the Johnson-Mehl-Avrami (JMA) [4, 5] transformation equation

$$x(t) = 1 - \exp(-Kt^n). \tag{4}$$

In this equation, the reaction rate constant K is a function of temperature, and, in general, depends on both the nucleation frequency and the crystal growth rate, and n is a parameter which reflects the nucleation frequency and/or the growth morphology.

The isothermal transformation rate $\mathrm{d}x(t)/\mathrm{d}t$ can be easily determined from Eq. (4) by differentiating with respect to time and substituting in the resulting expression the explicit relation between x and t given by Eq. (4) to yield

$$\frac{\mathrm{d}x}{\mathrm{d}t} = nK^{1/n}(1-x)\,[\ln(1-x)^{-1}]^{(n-1)/n}. \tag{5}$$

This equation is sometimes referred to as the Johnson-Mehl-Avrami transformation rate equation.

2.1 Evaluation of the Johnson-Mehl-Avrami transformation rate equation under conditions of continuous heating

It was suggested by Henderson [9] in a notable paper that Eq. (5) as developed by Johnson, Mehl and Avrami is based on the following important assumptions:

1. isothermal transformation conditions;
2. spatially random nucleation;
3. growth rate of new phase dependent only on temperature and not on time.

In the past decades the Eq. (5) has been applied without qualification to the analysis of non-isothermal phase transformations [10 to 12]. However, according to literature [13], the above-mentioned equation can be rigorously applied under non-isothermal conditions if it can be shown that the transformation rate depends only on the state variables x and T. Under this restriction an example of a system which allows the non-isothermal application of Eq. (5) is one in which the nucleation process takes place early in the transformation and the nucleation frequency is zero thereafter, which can be referred to as "site saturation" [14]. In addition, in the cases as the above mentioned, the reaction rate constant K could demonstrate a simple Arrhenius behaviour ($K = K_0 \exp(-E/RT_a)$) or a Vogel-Fulcher ($K = K_0 \exp[-E/R(T_a - T_0)]$ with respect to temperature during the crystallization process. In these expressions of the rate constant, K_0 is the frequency factor, E is the overall effective activation energy, R is the ideal gas constant, T_0 is a constant temperature, and T_a is the absolute temperature.

The analysis of crystallization kinetics is developed in terms of a generalized temperature parameter T. The generalized formalism can be applied directly to either Arrhenius behaviour or Vogel-Fulcher behaviour by substituting T_a or $T_a - T_0$ for T, respectively. Considering the generalized temperature dependence for K, the kinetic parameters associated with the transformation process are E, n, and K_0. The techniques of data analysis to obtain the quoted parameters can be divided into single-scan analysis and multiple-scan analysis techniques.

2.1.1 Single-scan technique

In the derivation of relationships for calculating kinetic parameters of the solid state transformations by using techniques of continuous heating, a reaction rate independent of the thermal history is necessary. Thus, the reaction rate is expressed as the product of two separable functions of absolute temperature and the fraction transformed. In these conditions the Eq. (5) can be written

$$\frac{\mathrm{d}x}{\mathrm{d}t} = nK^{1/n} f(x) = nK_0^{1/n} f(x)\,[\exp(-E/nRT)]\,. \tag{6}$$

Bearing in mind that the heating rate is $\beta = \mathrm{d}T/\mathrm{d}t$, the Eq. (6) must be integrated by separation of variables and one obtains

$$\int_0^x \frac{dx'}{(1-x')\,[\ln(1-x')^{-1}]^{(n-1)/n}} = \frac{nK_0^{1/n}}{\beta} \int_0^T e^{-E/nRT'}\,\mathrm{d}T' \tag{7}$$

and replacing $\ln(1-x')^{-1}$ with z' and E/nRT' with y', the integration of the Eq. (7) yields

$$[\ln(1-x)^{-1}]^{1/n} = K_0^{1/n} E(n\beta R)^{-1} \int_y^\infty \mathrm{e}^{-y'}\, y'^{-2}\,\mathrm{d}y' = K_0^{1/n} E(n\beta R)^{-1}\, I\,. \tag{8}$$

The integral I is not integrable in closed form and the literature [15, 16] gives several series expansions for the quoted integral. Vázquez et al. [17] have developed a method to evaluate it by an alternating series, resulting in

$$I = \left[-\mathrm{e}^{-y'}\, y'^{-2} \sum_{k=0}^{\infty} \frac{(-1)^k\,(k+1)!}{y'^k}\right]_y^\infty,$$

where it is possible to use only the two first terms, without making any appreciable error and to obtain

$$I = \left(\frac{nRT}{E}\right)^2 \left(1 - \frac{2nRT}{E}\right) \exp(-E/nRT)\,. \tag{9}$$

Substituting this expression of I in the Eq. (8), and taking the logarithm of the resulting expression gives

$$\ln\left[\ln(1-x)^{-1}\right] - 2n \ln T = -\frac{E}{RT} + n \ln \frac{nRK_0^{1/n}}{\beta E} \tag{10}$$

if it is assumed that the term $2nRT/E$ in Eq. (9) is negligible in comparison to unity, since in most crystallization reactions $E/RT \gg 1$ (usually $E/RT \geq 25$) [14]. When n is known, a plot of $\ln[\ln(1-x)^{-1}] - 2n \ln T$ versus $1/T$ yield a straight line whose slope gives a value of the activation energy. However, according to literature [18] over a temperature range of 100 K the contribution of T can be ignored without causing a substantial error in the calculated activation energy.

On the other hand, taking the logarithm of Eq. (6) results

$$\ln(\mathrm{d}x/\mathrm{d}t) = -\frac{E}{nRT} + \ln[f(x)] + \ln(nK_0^{1/n})\,. \tag{11}$$

Hence when $\ln(dx/dt)$ is plotted versus $1/T$ a straight line is obtained, whose slope allows to calculate the quotient E/n, if it is assumed that for $0.25 < x < 0.75$ the function $\ln[f(x)]$ may be considered as constant. The determination of E/n and E makes it possible to directly determine the parameter n.

For those systems in which K shows a Vogel-Fulcher temperature behaviour a determination of T_0 must also be made, according to Henderson [9]. In this case the effective activation energy, $E_{\text{eff}}(T_a)$, can be obtained by the relationship

$$\frac{d[\ln(dx/dt)]}{dT_a^{-1}} = \frac{E_{\text{eff}}(T_a)}{R} . \tag{12}$$

The derivative of Eq. (11) with respect to T_a^{-1} leads to the expression

$$\frac{d[\ln(dx/dt]}{dT_a^{-1}} = -\frac{E}{nR}\left(\frac{T_a}{T_a - T_0}\right)^2 - nK_0^{1/n}\,\frac{T_a^2}{\beta}\,\frac{df(x)}{dx}\,[\exp(-E/nRT)] .$$

Considering the negligible exponential term, and equating the resulting expression with Eq. (12), yields

$$E_{\text{eff}}(T_a)\,[(T_a - T_0)/T_a]^2 \approx -E/n = \text{const} ,$$

and measuring $E_{\text{eff}}(T_a)$ at two widely spaced temperatures T_{a1} and T_{a2}, the value of T_0 can be determined as

$$T_0 = (AT_{a1} - T_{a2})(A - 1)^{-1}$$

with $A = (T_{a2}T_{a1}^{-1})\{E_{\text{eff}}(T_{a1})[E_{\text{eff}}(T_{a2})]^{-1}\}^{1/2}$.

Finally, after E, n and T_0 have been determined, the frequency factor K_0 can be obtained by directly substituting for E and n in Eq. (6), yielding

$$K_0 = \left\{\frac{dx/dt}{nf(x)\,[\exp(-E/nRT)]}\right\}^n . \tag{13}$$

2.1.2 Multiple-scan technique

The single-scan analysis techniques outlined above is predicated on a detailed knowledge of the functional dependence of the transformation rate dx/dt on the fraction transformed x and the generalized temperature T. The multiple-scan rate analysis techniques do not depend on a specific knowledge of the dependence of dx/dt on x. The procedure requires the characterization of the transformation by using several different scan rates. When this procedure is applied to the case of a JMA transformation rate equation, generalization of Eq. (4) for the treatment of continuous heating experiments is interesting. If it is assumed that the transformation products and mechanism do not change with temperature, then it is reasonable to replace $K^{1/n}t$ with $\int_0^t [K(T(t'))]^{1/n}\,dt'$, according to literature [19], and Eq. (4) generalizes to

$$x(t) = 1 - \exp\left\{-\left[\int_0^t [K(T(t'))]^{1/n}\,dt'\right]^n\right\} = 1 - \exp\left(-I_1^n\right) , \tag{14}$$

where $K(T(t')) = K_0 \exp(-E/RT)$ and $T(t')$ is the above-mentioned generalized temperature. The maximum transformation rate is found by making $d^2x/dt^2 = 0$, thus ob-

taining the relationship

$$nK_p^{1/n}\left(I_1^n\right)\big|_p = \beta E I_1|_p (nRT_p^2)^{-1} + (n-1)\,K_p^{1/n}\,, \tag{15}$$

where the magnitude values which correspond to the maximum crystallization rate are denoted by subscript p. Replacing E/nRT' by y', the integral I_1 is expressed as a function of the integral I, which can be evaluated [17] as in Section 2.1.1, yielding an expression for $I_1|_p$, that when is inserted in Eq. (15) results in $I_1|_p = (1 - 2RT_p/E)^{1/n}$. When both expressions for $I_1|_p$ are equated, one obtains a relationship whose logarithmic form can be written as

$$\ln\left(T_p^2/\beta\right) + \ln\left(nRK_0^{1/n}/E\right) - E/nRT_p \approx \left(2nRT_p/E\right)\left(1 - 1/n^2\right), \tag{16}$$

where the function $\ln(1 - v)$ with $v = 2RT_p/E$ or $v = 2nRT_p/E$ is expanded as a series and has been taken only the first term of itself.

Note that, for most crystallization reactions, the right-hand side (RHS) of Eq. (16) is generally negligible in comparison to the individual terms on the left-hand side for common heating rates ($\leq$100 K min^{-1}), thus for $n > 1$ and $E/RT_p > 25$ the error introduced in the value of E/nR is less than 1%. Equation (16) serves to determine the quotient E/n and the frequency factor K_0 from the slope and intercept, respectively, of the $\ln(T_p^2/\beta)$ versus $1/T_p$ plot.

Finally, it should be noted that Eq. (16) with RHS = 0 is obtained, considering that $2RT_p/E \ll 1$, according to literature [14], and therefore, $I_1|_p = 1$, $K_p^{1/n} = \beta E(RT_p^2)^{-1}$ and considering the expression for $(\mathrm{d}x/\mathrm{d}t)|_p$ results

$$E = RT_p^2(\mathrm{d}x/\mathrm{d}t)|_p\,(0.37\beta)^{-1}\,. \tag{17}$$

This equation permits to calculate the kinetic parameter E in a set of exotherms taken at different heating rates and the corresponding mean value represents the overall activation energy of the crystallization process.

3. Experimental Procedures

The semiconducting $Sb_{0.12}As_{0.40}Se_{0.48}$ glass was made in bulk form, from their components of 99.999% purity, which were pulverized to less than 64 μm, mixed in adequated proportions, and introduced into quartz ampoules. The ampoules were subjected to an alternating process of filling and vacuuming of inert gas, in order to ensure the absence of oxygen inside. This ended with a final vacuuming process of up to 10^{-4} Torr (10^{-2} Nm^{-2}), and sealing with an oxyacetylene burner. The ampoules were put into a furnace at around 1225 K for 24 h, turning at 1/3 r.p.m., in order to ensure the homogeneity of the molten material, and then quenched in water to avoid crystallization. The capsules containing the samples were then put into a mixture of hydrofluoridic acid and hydrogen peroxide in order to corrode the quartz and make it easier to extract the alloy. The glassy nature of the material was confirmed by a diffractometric X-ray scan, in a Siemens D500 diffractometer, showing the absence of peaks which are characteristic of crystalline phases. The homogeneity and composition of the samples were verified through SEM in a Jeol, scanning microscope JSM-820. The calorimetric measurements were carried out in a Perkin-Elmer DSC7 differential scanning calorimeter with an accuracy of ±0.1 K, keeping a constant flow of nitrogen in order to extract the gases

generated during the crystallization reactions, which, as is characteristic of chalcogenide materials, are highly corrosive for the DSC sensor equipment. The calorimeter was calibrated, for each heating rate, using the well-known melting temperatures and melting enthalpies of high purity zinc and indium supplied with the instrument. The analyzed samples were pulverized (particle size around 40 μm), crimped into aluminium pans, and their masses were kept about 20 mg. An empty aluminium pan was used as reference. The crystallization experiments were carried out through continuous heating at rates β of 2, 4, 8, 16, 32 and 64 K min^{-1}. The glass transition temperature was considered as a temperature corresponding to the inflection point of the lambda-like trace on the DSC scan, as shown in Fig. 1.

4. Results and Discussion

The DSC curve of alloy under study obtained at a heating rate of 4 K min^{-1} and plotted in Fig.1 makes it possible to determine the glass transition temperature, $T_g = 474$ K, the extrapolated onset crystallization temperature, $T_c = 569$ K, and the peak temperature of crystallization, $T_p = 587$ K, of the above-mentioned alloy. This DSC trace shows the typical behaviour of a glass–crystal transformation. The DSC registers for the different heating rates β, quoted in Section 3, show values T_g, T_c and T_p which increase with increasing β, a property which has been widely quoted in the literature [20].

4.1 The crystallization

The kinetic analysis of the crystallization reactions is related with the knowledge of the reaction rate constant as a function of temperature. In the present work it is assumed that the above-mentioned constant shows an Arrhenius-type temperature dependence. In order for this assumption to hold, according to literature [20], one of the following two sets of conditions should apply:

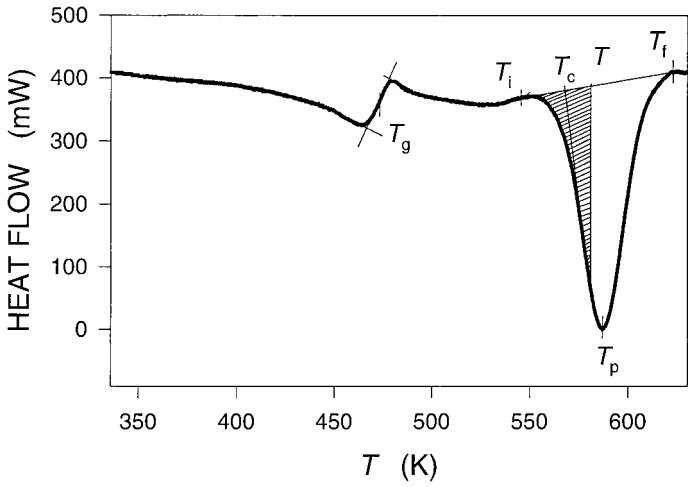

Fig. 1. Typical DSC trace of $Sb_{0.12}As_{0.40}Se_{0.48}$ glassy alloy at a heating rate of 4 K min^{-1}. The hatched area shows A_T, the area between T_i and T

Table 1
The characteristic temperatures and enthalpies of the crystallization processes of alloy $Sb_{0.12}As_{0.40}Se_{0.48}$

parameter	experimental value
T_g (K)	459.2 to 490.9
T_i (K)	534.7 to 579.8
T_p (K)	579.3 to 641.4
ΔT (K)	51.1 to 73.0
ΔH (mcal mg^{-1})	4.1 to 5.1

(i) The crystal growth rate u has an Arrhenius-type temperature dependence; and over the temperature range where the thermoanalytical measurements are carried out, the nucleation rate is negligible (i.e. the condition of "site saturation").

(ii) Both the crystal growth and the nucleation frequency have Arrhenius-type temperature dependences.

In this work the first condition is assumed in order to apply the JMA equation under conditions of continuous heating. From this point of view, the crystallization kinetics of the $Sb_{0.12}As_{0.40}Se_{0.48}$ alloy has been analyzed by using the calorimetric techniques of single-scan and multiple-scan.

With the aim of analyzing the above-mentioned kinetics, the variation intervals of the magnitudes described by the thermograms for the different heating rates, quoted in Section 3, are obtained and given in Table 1, where T_i and T_p are the temperatures at which crystallization begins and that corresponding to the maximum crystallization rate, respectively, and ΔT is the width of the peak. The crystallization enthalpy ΔH is also determined for each heating rate. The crystallization rates corresponding to the different scans are represented in Fig. 2. It may be observed that the $(dx/dt)_p$ values increase in the same proportion as the heating rate, a property which has been widely discussed in the literature [20].

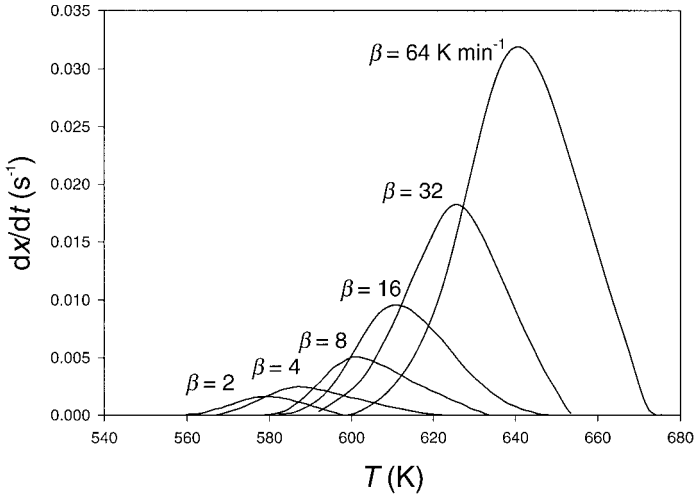

Fig. 2. Crystallization rate versus temperature of the exothermal peaks at different heating rates

Table 2
Kinetic parameters found for the crystallization of the $Sb_{0.12}As_{0.40}Se_{0.48}$ alloy by using the single-scan and multiple-scan techniques

β (K/min)	single-scan					multiple-scan					
	interval		E (kcal/mol)	E/n (kcal/mol)	n	K_0 (s^{-1})	T_p (K)	$10^3 (dx/dt)_p$ (s^{-1})	E (kcal/mol)	E/n (kcal/mol)	n	K_0 (s^{-1})
	T (K)	$10^3 (dx/dt)_p$ (s^{-1})										
2	569.1 to 578.2	0.78 to 1.33	76.8	38.4	2.00	1.73×10^{23}	579.3	1.37	74.4			
4	577.2 to 586.8	1.49 to 2.48	71.9	36.1	1.99	3.87×10^{21}	587.0	2.48	69.4			
8	588.1 to 597.7	2.68 to 4.58	78.1	39.3	1.99	7.73×10^{23}	601.4	5.18	76.0	38.5	1.88	1.31×10^{22}
16	604.5 to 610.3	6.82 to 9.21	76.6	38.3	2.00	2.33×10^{23}	610.9	9.80	74.2			
32	614.7 to 623.8	11.23 to 17.46	75.2	37.2	2.02	5.99×10^{22}	625.8	18.26	72.5			
64	628.7 to 639.0	20.61 to 32.08	69.4	34.5	2.01	5.43×10^{20}	641.4	32.43	67.7			

The single-scan technique was applied to several sets of experimental data (Table 2) obtained for all heating rates, quoted in Section 3, and the results for E from Eq. (10), E/n from Eq. (11), n derived therefrom and K_0 are included in Table 2. The mean values for these parameters are: $\langle E \rangle = 74.7$ kcal mol^{-1}, $\langle n \rangle = 2$ and $\langle K_0 \rangle = 2.07 \times 10^{23}$ s^{-1}. To illustrate the above-mentioned technique, Fig. 3 shows the plots of $\ln[-\ln(1-x)]$ versus $1/T$ for $\beta = 16$ K min^{-1}, together with the corresponding straight regression line, while the plots of $\ln(dx/dt)$ versus $1/T$ with the straight regression line carried out, are shown in Fig. 4.

On the other hand, the multiple-scan technique, which allows E/n to be quickly evaluated, has been used to analyze the crystallization kinetics of the semiconducting $Sb_{0.12}As_{0.40}Se_{0.48}$ alloy. The plots of $\ln(T_p^2/\beta)$ versus $1/T_p$ at each heating rate, and the straight regression line carried out are shown in Fig. 5. The results for E/n and K_0 from Eq. (16) are given in Table 2.

By using the values of the maximum crystallization rate, and the temperatures, which correspond to the quoted maximum values, given in Table 2, it is possible to obtain, through Eq. (17), the activation energy of the process corresponding to each of experimental heating rates. The values of the parameter E are also shown in above-mentioned Table 2. Bearing in mind that the calorimetric analysis is an indirect method which makes it possible to obtain mean values for the parameters that control the kinetics of a reaction, the corresponding mean value, $\langle E \rangle = 72.4$ kcal mol^{-1}, has been calculated. Once the values of E/n and E were known, the value of kinetic exponent, $n = 1.88$, was immediately obtained.

With the aim of correctly analyzing the reliability of the single-scan technique, when calculating kinetic parameters in non-isothermal crystallization processes, the above parameters E, n and $\ln K_0$, calculated by means the above-mentioned technique, are compared with its values obtained through the multiple-scan technique, Table 2, finding that the error between them for the less accurate parameter is less than 6%. This

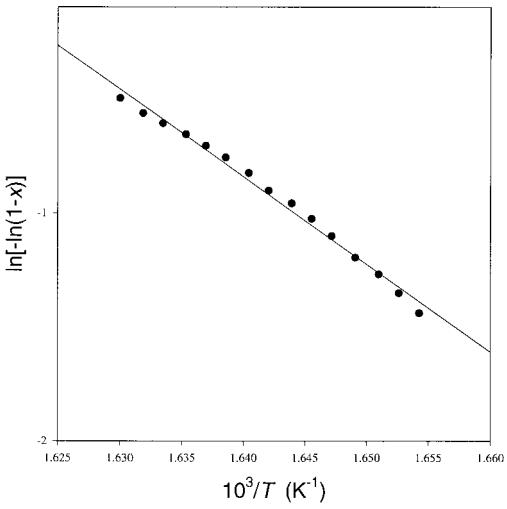

Fig. 3. Variation of $\ln[-\ln(1-x)]$ with $1/T$ for a heating rate of 16 K min^{-1}

result is in agreement with the literature [12], where is shown that for $(n-1)/n = 0.6$ in the range of $0.2 < x < 0.4$ it results in an error of 7% in the calculated slope E/R, an error acceptable in most crystallization reactions.

Considering that the crystallization process of the studied material is basically a growth of the pre-existing nuclei in the as-quenched glass, from the value of the kinetic exponent $n = 2$, and according to the Avrami theory of crystal growth, it is possible to state the fact that in the crystallization reaction mechanism there is a diffusion-controlled growth, coherent with the basic formalism used. According to the literature [21] the transformed phase may exhibit an initial growth of particles nucleated at a constant rate, since the mean value of the kinetic exponent is included in the interval 1.5 to 2.5.

For the unambiguous interpretation of $n \approx 2$ as a consequence of a diffusion-controlled crystallization, it is recommended to try to identify the possible phases that crystallize in the material after the thermal treatment by means of adequate X-ray diffraction measurements. The diffractograms for as-quenched glass and for the material after the overall crystallization are shown in Fig.6. Figure 6a shows broad humps characteristic of the amorphous state of the starting material. The diffractogram of the transformed material suggests the presence of microcrystallites of Sb_2Se_3 and AsSe indicated

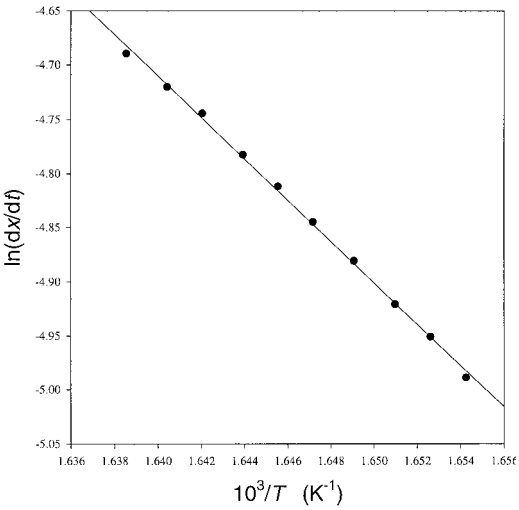

Fig. 4. Experimental plots of $\ln(dx/dt)$ versus $1/T$ and straight regression line of the $Sb_{0.12}As_{0.40}Se_{0.48}$ alloy

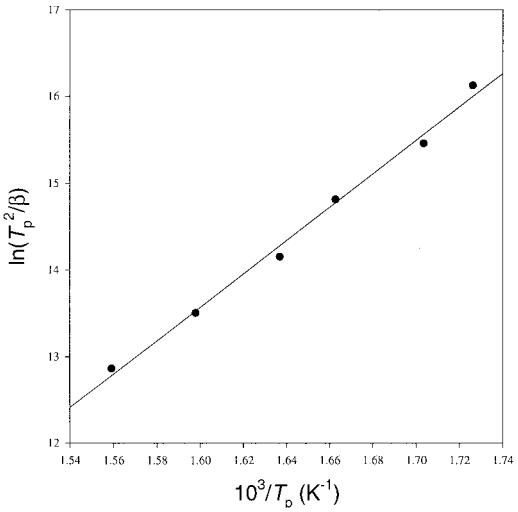

Fig. 5. Plots of ln (T_p^2/β) versus $1/T_p$ of the analyzed material

Fig. 6b with solid and open circles, respectively. The Sb_2Se_3 phase found crystallizes in the orthorhombic system [22] with a unit cell defined by a = 11.633 Å, b = 11.78 Å and c = 3.895 Å.

5. Conclusions

The described theoretical procedure enables us to study the evolution with time of the volume fraction transformed in materials involving nucleation and crystal growth processes. This method assumes the concept of the extended volume in transformed material and the condition of random nucleation. Using these assumptions, a general expression for the transformed fraction as a function of time in

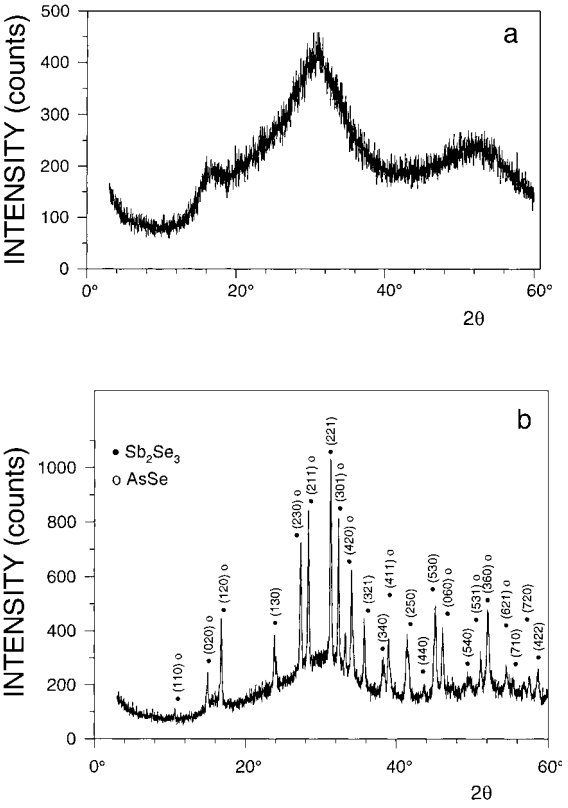

Fig. 6. a) Diffractogram of the amorphous $Sb_{0.12}As_{0.40}Se_{0.48}$alloy, b) diffraction peaks of the alloy crystallized in DSC

bulk crystallization processes has been obtained. In the case of isothermal crystallization, the above-mentioned expression has been transformed in an equation, which can be taken as a specific case of the JMA transformation equation. The application of this equation to non-isothermal transformations implies restrictive conditions, as it is the case of a transformation rate which depends only on the fraction transformed and the temperature. Under this restriction the kinetic parameters have been deduced both for the single-scan technique and for the multiple-scan techniques, which are applicable to constant scan rate DTA and DSC experiments on materials which obey the JMA transformation rate equation.

The above-mentioned techniques have been applied to the crystallization kinetics of the semiconducting $Sb_{0.12}As_{0.40}Se_{0.48}$ alloy. The difference between the obtained values for the kinetic parameters by means of both techniques is less than 6%. This good agreement shows the reliability of the single-scan technique for the calculation of kinetic parameters, mainly in the interval 0.2 to 0.5 of the volume fraction crystallized, a fact in agreement with the literature.

Acknowledgements The authors are grateful to the Junta de Andalucía and the CICYT (Comisión Interministerial de Ciencia y Tecnología, project No. MAT 98-0791) for their financial supports.

References

[1] Z. Altounian and J. O. Strom-Olsen, Thermal Analysis in Metallurgy, Eds. R. D. Shull and A. Joshi, The Minerals, Metals and Materials Society, Warrendale, P.A. 1992 (p. 155).
[2] K. F. Kelton, Crystal Nucleation in Liquids and Glasses, Solid State Physics, Vol. 45, Academic Press, New York 1991.
[3] N. Clavaguera, J. Non-Cryst. Solids **162**, 40 (1993).
[4] M. Avrami, J. Chem. Phys. **7**, 1103 (1939); **8**, 212 (1940); **9**, 177 (1941).
[5] W. C. Weinberg and R. Kapral, J. Chem. Phys. **91**, 7146 (1989).
[6] M. P. Shepilov and D. S. Baik, J. Non-Cryst. Solids **171,** 141 (1994).
[7] V. Erukhimovitch and J. Baram, J. Non-Cryst. Solids **208,** 288 (1996).
[8] J. Vázquez, P. Villares, and R. Jiménez-Garay, J. Alloys and Comp. **257**, 259 (1997).
[9] D. W. Henderson, J. Non-Cryst. Solids **30**, 301 (1979).
[10] F. Skvara and V. Satava, J. Therm. Anal. **2,** 325 (1970).
[11] J. Sestak, Thermochim. Acta **3**, 1 (1971).
[12] J. Sestak, Phys. Chem. Glasses **6**, 137 (1974).
[13] T. Keméný, Thermochim. Acta **110**, 131 (1987).
[14] J. Vázquez, C. Wagner, P. Villares, and R. Jiménez-Garay, J. Non-Cryst. Solids **235/237,** 548 (1998).
[15] P. Murray and J. White, Trans. Brit. Ceram. Soc. **54**, 204 (1955).
[16] C. D. Doyle, Nature **207**, 290 (1965).
[17] J. Vázquez, C. Wagner, P. Villares, and R. Jiménez-Garay, Acta Mater. **44**, 4807 (1996).
[18] J. Sestak, Thermochim. Acta **3**, 150 (1971).
[19] J. Vázquez, P. L. López-Alemany, P. Villares, and R. Jiménez-Garay, J. Alloys and Comp. **270**, 179 (1998).
[20] J. Vázquez, P. L. López-Alemany, P. Villares, and R. Jiménez-Garay, Mater. Chem. Phys. **57**, 162 (1998).
[21] C. N. R. Rao and K.J. Rao, Phase Transition in Solids, Mc Graw Hill, New York 1978.
[22] S. A. Demboski, Russ J. Inorg. Chem. (Engl. transl.) **8**, 798 (1963).